Optimal Range and Doppler Centroid Estimation for a ScanSAR System

Michael Y. Jin

Jet Propulsion Laboratory
California Institute of Technology
Pasadena, California 91109, USA

PHONE: (81 8) 354-3778

TELEFAX: (818) 393-6943

E-MAIL: michael_jin@radar-email.jpl.nasa.gov

The research described in this paper was carried out by the Jet Propulsion Laboratory, California Institute of Technology, under a Contract with the National Aeronautics and Space Administration.

Optimal Range and Doppler Centroid Estimation for a ScanSAR System

Michael Y. Jin

Jet Propulsion Laboratory
California Institute of Technology
Pasadena, California 91109, USA

Abstract

This paper presents a new range and Doppler centroid estimation algorithm for a ScanSAR system. Its accurate range and Doppler centroid estimates lead to refined radar pointing angles, which enables the ScanSAR imagery meeting its radiometric requirements. This algorithm attains an accuracy equal to the Cramer Rae's lower bound for both the homogeneous and quasi-homogeneous targets. This algorithm is also efficient in computation and easy for implementation.

1. INTRODUCTION

An accurate radar pointing is often required in SAR processing in order to meet its radiometric accuracy and signal-to-ambiguity requirements. However, the attitude control unit in most SAR systems can not provide such an accurate data. An alternative approach to solve this problem is to derive the pointing angles from the SAR data by estimating the range and Doppler centroids. Available methods include clut terlock techniques [1,2,3] and multiple PRF techniques [4] to improve the azimuth pointing accuracy; and the range centroid tracking technique [5] to improve the elevation pointing accuracy.

In processing a ScanSAR data, error in the radar pointing leads to a variation of the image intensity in azimuth. To meet the radiometric accuracy requirement, it would require an azimuth pointing angle much more accurate than that required for a strip mode SAR [6]. Therefore, estimation for range and Doppler centroid is a more challenging problem to a ScanSAR system. Unfortunately, all available clutterlock algorithms [1, 2, 3] are not applicable or best suitable to a ScanSAR system since they were devised for the strip mode system.

In this paper, a new range and Doppler centroid estimation algorithm is presented. This algorithm is based on the idea of using the overlap regions between adjacent beams or adjacent bursts [7]. In particular, the range or Doppler centroid is obtained from the estimate of the range or Doppler value at which the intensities of two adjacent images are crossing over each other. Since this algorithm is scene independent, it achieves the same accuracy for both the homogeneous and quasi-homogeneous targets, without special treatment for the later [2].

For the RADARSAT ScanSAR, this algorithm will lead to highly accurate radar pointing angles to be able to meet the stringent radiometric requirement of the RADARSAT system. In addition, the Doppler centroids obtained from two adjacent beams would be accurate enough for resolving the PRF ambiguity based on the two different PRFs selected for the two beams. This may reduce the software development effort of implementing other types of PRF ambiguity determination algorithm and enhance the successful rate of resolving the PRF ambiguity for a ScanSAR processor system.

2. EFFECT OF POINTING ERROR ON SCANSAR IMAGE

Each ScanSAR burst processed by a traditional SPECAN (or deramp-FFT) algorithm results in a range-Doppler image. The intensity of this image is modulated by a two -dimensional antenna pattern and the reciprocal of the cubic of the slant range . In order to derive the backscattering coefficient of the ground target, proper removal of the antenna pattern and the slant range variation is necessary. In this process, error in the antenna pointing angles would skew the antenna pattern reference and cause a intensity ramp modulation, as shown in Fig. 1, in the final burst image. Overlaying these intensity distorted burst images, in the projection domain, would generate an image with an intensity variation in both range (due to multiple beams) and azimuth dimensions.

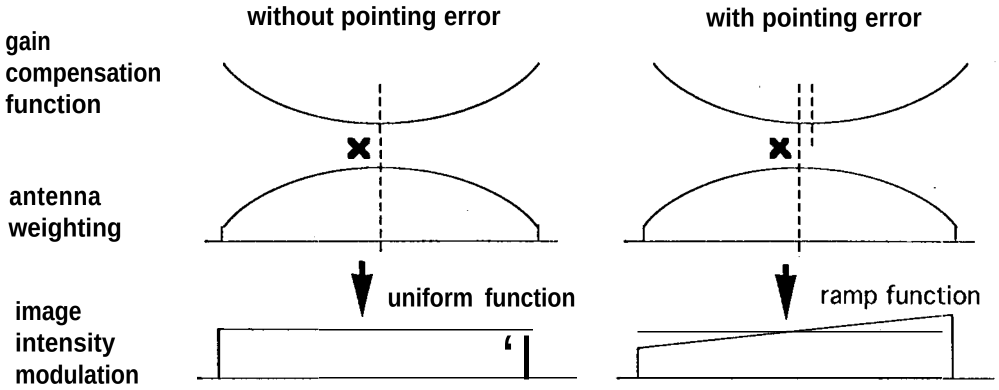

Figure 1. Effect of Pointing Error on Image Intesity

in RADARSAT ScanSAR system, the requirement of the relative radiometric error is 0.5 dB. A common radiometric error budget may also have an allocation to error contributed by the processor. This includes error in modeling the antenna pattern and error in the amount of attitude drift within the interval of pointing angle updates. This results in a very stringent requirement on the intensity variation in both range and azimuth dimensions. Assuming that the allocation to the image intensity variation is only 0.25 dB, the required azimuth pointing accuracy would be - 0.0035^{o} (or 25 Hz). This impose a more stringent requirement on the azimuth pointing estimation than that of a strip mode SAR system.

To estimate the pointing angle, one can utilize the range-Doppler images before any radiometric compensation is applied, This idea can be illustrated by Figure 2. Depicted in this Figure are the intensity functions of two adjacent burst images (of the same beam or adjacent beams) with homogeneous targets; x_1 and x2 are the projection coordinates (in either range or azimuth) of the center of antenna illumination in images processed from two adjacent bursts; and xc is the coordinate at which the intensities of both images are equal. Obviously, x_1 and x2 are determined by the radar pointing angle. Since the distances of $x_c x_1$ and $x_c x_2$ are fixed, one can obtain the value of x_1 or the radar pointing angle by estimating the value of xc. This idea leads to the optimal ratio algorithm described below.

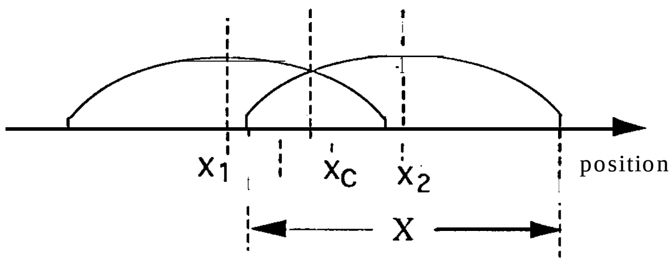

Figure 2. Intensity functions of two adjacent burst images

3. OPTIMAL RATIO ALGORITHM

Having a radiometric compensation for the slant range variation, the intensity of a range-Doppler image in a ground projection can be expressed as a two-dimensional function of the positions x and y in the following form:

$$I(x, y) = W(x - x_0, y - y_0) \cdot \sigma(x, y) \cdot \gamma(x, y) \tag{1}$$

where $W(x - x_0, y - y_0)$ is the antenna pattern centered at x_0 and y., $\sigma(x, y)$ is the backscattering coefficient of the scene, and $\gamma(x, y)$ is the random process of the radar speckle with an exponential distribution. Without loss of generosity, we will now consider a one-dimensional intensity function only. For two adjacent bursts, the intensities of their range-Doppler images in ground projection can be expressed as

$$I_1(x) = W_1(x - x_1) \cdot \sigma(x) \cdot \gamma_1(x) \quad \text{for} \quad x_1 - X/2 \le x \le x_1 + X/2$$
$$\text{and} \quad I_2(x) = W_2(x - x_2) \cdot \sigma(x) \cdot \gamma_2(x) \quad \text{for} \quad x_2 - X/2 \le x \le x_2 + X/2 \tag{2}$$

where X is the size of the image. Equation (2) is a general case which have two different antenna patterns, one for each burst image. For Doppler centroid estimation, only one antenna pattern is required because it is shared by both burst images. Since the backscattering coefficient function $\sigma(x)$ is unknown and not predictable, it is desirable to cancel this factor by taking the ratio of 11(x) and 12(x). Assuming that $x_1 < x2$, this ratio is given by

$$r(x) = \frac{W_1(x - x_1)}{W_2(x - x_2)} \cdot \frac{\gamma_1(x)}{\gamma_2(x)} \quad \text{for} \quad x_2 - X/2 \le x \le x_1 + X/2 \tag{3}$$

To detect the intensity cross-over point xc, one may suggest a matching technique to correlate the intensity ratio function with the ratio of the antenna pattern in order to reduce the effect caused by the speckle noise. There are two problems associated with this method. One is that the ratio of the two random processes is extremely noisy. The mean and variance of its sample are not bounded. Second, the ratio of the antenna pattern is quite unbalanced; one end toward a value much greater than one while the other end being much smaller than one. Both problems prevent getting a reliable estimate of xc.

A simple solution to these problems is to take the logarithm of the intensity ratio first. This changes the speckle noise from multiplicative to additive and also changes the ratio of the antenna pattern from extremely unbalanced to well balanced. Denote the nature logarithm of the ratio by $R(x)$, it has the following form:

$$\begin{aligned} R(x) &= \log\left(W_1(x - x_1)/W_2(x - x_2)\right) + \log\left(\gamma_1(x)/\gamma_2(x)\right) \\ &= A(x - \mathrm{Xc}) + \beta(x) \end{aligned} \tag{4}$$

where $\beta(x)$ denotes $\log(\gamma_1(x)/ 7_2(x))$. It can be shown that $\beta(x)$ is a much well behaved random process with a mean of zero and a variance of 3.29. One may average this logarithm ratio function in the y dimension to further reduce the noise. By doing so, the noise component $\beta(x)$ become Gaussian distributed, Hence, one can apply the matching technique described in [8] to get a maximum likelihood estimate of xc. The accuracy of this technique is equal to the Cramer Rae's lower bound. Its processing steps include: (1) to convolve R(x) with the first order derivative of $A(x - x_c)$, and (2) to detect the zero-crossing point over the interval of $(x_2 - X/2, \mathrm{Xl} + X/2)$.

4 CRAMER RAO'S LOWER BOUND

For any estimation problem, it is desirable to examine its performance by comparing its variance with the Cramer Rae's lower bound. In order to do so, we rewrite equation (4) in a discrete form as

$$R(i) = A(i \cdot \delta x - x_c) + \beta(i) \qquad \text{for} \qquad -\Delta x_1 \le i \cdot \delta x - x_c \le \Delta x_2 \tag{5}$$

where δx is the sampling spacing, Δx_1 and Δx_2 are the distances between the intensity cross-over point and each end of the overlap. We shall assume that the sampling rate is equal to the Nyquist rate. Consider that $R(i)$ is the result of average in the y dimension, therefore, it is Gaussian distributed with a mean value of $A(i \cdot \delta x - x_c)$. The variance of $\beta(i)$ is then equal to $3.29/N_l$, where N_l is the number of lines taken for average. The joint probability density function can be formed as

$$p(R(1), R(2), \ldots, R(n_s)) = \prod_{i=1}^{n_s} \frac{1}{\sqrt{2\pi}\sigma} \cdot \exp\left\{ \frac{JR(i) - A(i.\ \delta x - x_c))^2}{2\sigma^2} \right\} \tag{6}$$

where n_s is the number of samples in $(x_c - \Delta x_1, x_c + \Delta x_2)$. The Cramer-Rao inequality [9] states that the variance of any (unbiased) position x_c estimate is bounded by

$$\mathrm{var}\{x_c\} \geq \frac{1}{E\left\{\left(\frac{\partial \ln p(R; x_c)}{\partial x_c}\right)^2\right\}} \tag{7}$$

Based upon equation (6) and (7), The lower bound of the variance of xc can be found to be

$$\mathrm{var}\{x_c\} \geq \mathrm{var}\{\beta(k)\} \cdot \delta x \frac{1}{\int_{-\Delta x_1}^{\Delta x_2} [A'(x - x_c)]^2 dx} = \frac{3.29 \cdot N_l^{-1} . \delta.}{\int_{-\Delta x_1}^{\Delta x_2} [A'(x - x_c)]^2 dx} \tag{8}$$

A more rigorous derivation of the Cramer-Rae's lower bound can be obtained by forming the joint probability density function of $R(i)$ that is not averaged in the y dimension. The result is very close to that of (8). This derivation is given in Appendix A.

4.1 Cramer Rae's Lower Bound for Doppler Centroid Estimate

Let $W_a(f)$ be the azimuth antenna pattern as a function of the Doppler frequency f, Af be the interval of the Doppler frequency corresponding to the overlap of two burst images, and δf be the Doppler sample spacing. For a Doppler centroid estimate made from N_l lines, its Cramer Rae's lower bound is given by

$$\mathrm{var}\{ f_{dc} \} \geq \frac{3.29 \cdot N_l^{-1} . \delta f}{\int_{-\Delta f/2}^{\Delta f/2} \left(\frac{W'_a(f + \Delta f/2)\ W'_a(f - \Delta f/2)}{W_a(f + \Delta f/2)\ W_a(f - \Delta f/2)} \right)^2 dx} \tag{9}$$

We can further express the standard deviation of the Doppler centroid estimate by

$$SD\{f_{dc}\} = C_1 \ (\Delta f) \cdot \frac{PRF}{\sqrt{N_l \cdot n_s}}$$

where PRF is the pulse repetition frequency, n_s = Af / δf, and C_1 (Af) is a coefficient determined by the integral in (9) and the value of Af. Table 1 lists the value of C_1 (Af) and its corresponding Af.

Table 1. C_1(Δf) and Af of the Optimal ratio Algorithm

Δf/PRF	.125	,25	.375	.50	.625	.75	.875
C_1(Δf)	.80	.33	.244	.233	.259	.326	,50

This Table indicates that at 50% overlap of the Doppler spectrum, this algorithm is most accurate. Increasing or decreasing the amount of overlap reduces the accuracy. To be noted is that the coefficient from optimal algorithm for a strip mode SAR is 0.2516 [2, 10]. One can see that some of the cases in Table 1 are even better. This does not imply that by estimating the Doppler centroid using all the SAR data acquired over a target area would yield better accuracy than that of [2, 10] because in a ScanSAR there is a lack of data between bursts. For a ScanSAR system with more than two azimuth looks, one can optimally combine the Doppler centroid estimates obtained from all pairs of bursts within the interval of a f ull apert ure by using weights formed based upon their C_1 (Af) coefficients.

4.2 Cramer Rae's Lower Bound for Range Centroid Estimate

A simple form of (8) can be obtained under two conditions: (1) one has the knowledge of the gain difference of the two antenna functions, W_1 $(x - x_1)$ and $W_2(x -$ x2), at the edge of overlap, and (2) the function of $A'(x - x_c)$ is approximately a constant. For RADARSAT ScanSAR system, both assumptions are valid. Denote Δg_1 and Ag_2 as the absolute gain difference at each end of the overlap in dB unit, the simplified form is given by

$$\mathrm{var}\{x_c\} \geq \frac{61.64 \cdot (\Delta g_1 + \Delta g_2)^{-2} . \delta x^2 \cdot n_s}{N_l} \quad (1o)$$

This form is particularly useful for estimating the variance of the range centroid estimate since one dots not have to deal with any of the many pairs of antenna patterns in a multiple beam ScanSAR. The following example is given to illustrate the use of (10), An estimate of the range centroid is made from 64 lines with 1024 samples in the overlap, The ground range sample spacing is 30 meter and the absolute gain difference of the two antenna functions at each edge of overlap is 10 dB. By inserting these numbers into (1 O), the standard deviation of the range centroid estimate is found to be 47 meter. For a SAR at 800 km altitude with 20° incidence angle, the corresponding elevation angle has a standard deviation of 0.003°.

5. NOISE AND AMBIGUITY EFFECTS

Two problems are often encountered in range and Doppler centroid estimate. These are the system noise and the ambiguities of both range and azimuth. The system noise is different from the speckle noise and is primarily the combination of the thermal noise existed in front of the analog-to-digital conversion circuit and the quantization noise after the analog-to-digital conversion. For a homogeneous target, one can further optimize the centroid estimates by adding to the antenna pattern a constant, derived from the signal-to-noise (SNR) estimate, to form the weighting function for searching the intensity cross-over point. For a quasi-homogenous target with a good SNR (>1 O db), the centroid estimation algorithm and its lower bound given in the previous sections are both applicable and accurate. For a relatively poor SNR, the performance of this algorithm will be degraded.

The range and azimuth ambiguities are the ghost images caused by the antenna sidelobes. In a SAR system design, the ambiguity level is usually low enough to show any visible ambiguities from neighboring scenes of comparable intensity. However, for neighboring scenes with a much higher intensity, its ambiguity significantly degrades the centroid estimate. The algorithm to suppress the ambiguities given in [11] can be modified and used for a ScanSAR processor in order to achieve higher image quality as well as more accurate centroid estimate.

6. DISCUSSION

The Doppler centroid estimation algorithm described here can also be applied to a strip mode SAR. It has two advantages: (1) this algorithm is more efficient in computation and (2) it does not suffer performance degradation from a quasi-homogeneous target. The computation efficiency is due to the facts that in forming a range-Doppler image, it involves less computation per output pixel than a strip mode correlation process. In addition, since a very high Doppler centroid accuracy is usually not required, a conventional strip mode SAR Doppler centroid estimator has its trade-off between the amount of computation and the range processing bandwidth. In this ScanSAR type Doppler centroid estimation process, the trade-off for the amount of computation is simply the number of pulses in a burst, This trade-off is also more effective than that of the strip mode.

To implement this centroid estimation algorithm in a ScanSAR processor, it is relatively complicated to convert the range-Doppler image into the projection domain and convert them back to the range-Doppler domain after the averaged logarithm rat io function is formed. To solve this problem, one can substitute the projection coordinate by the range-Doppler coordinate of the first burst. Then, for each target one need to relate the range-Doppler pair of the second burst to that of the first one by

$$\begin{aligned} r_2 &= r_1 - \frac{\lambda}{2}\left(f_{d1} \cdot t_p + \frac{1}{2} f_r \cdot t_p^2\right) \\ f_{d2} &= f_{d1} + f_r \cdot t_p \end{aligned} \qquad (11)$$

where r_1, f_{d1} and r_2, f_{d2} are the range Doppler of the two bursts, f_r is the Doppler frequency rate, and t_p is the time difference between the second burst and the first burst. This coordinate will greatly simplify the estimation process.

7. SUMMARY

An accurate and efficient range and Doppler centroid estimation algorithm is presented in this paper. The accuracy of this estimator is equal to the Cramer Rae's lower bound. This algorithm provides the same high accuracy for both the homogeneous target and the quasi-homogeneous target. Estimation process can be further simplified by choosing proper coordinate. This algorithm will be very useful for the RADARSAT ScanSAR and for all future ScanSAR systems. This algorithm is also a very good candidate for Doppler centroid estimation of a strip mode SAR.

ACKNOWLEDGMENTS

The research described in this paper was carried out by the Jet Propulsion Laboratory, California Institute of Technology, under a Contract with the National Aeronautics and Space Administration.

APPENDIX A

Now consider that $R(i)$ is not averaged in the y dimension and the random variables $\beta(i)$, $i=$ 1,2, ... n_s, are not Gaussian distributed. Because the mean of $\beta(i)$ is zero, the pdf of $R(i)$ can be written as $f(R(i)-A(i.\ \delta x - x_c))$. Since h?(1), R(2),..., and $R(n_s)$ are independent of each other, their joint pdf can be formed as

$$p(R(1),R(2),\ldots,R(n_s))=\prod_{i=1}^{n_s} f(R(i)-A(i\cdot \delta x - xc)) \tag{al}$$

The first order derivative of the maximum likelihood function of the joint pdf by x_c can be obtained as

$$\frac{\partial \ln p(\boldsymbol{R};x_c)}{\partial x_c}=\sum_{i=1}^{n_s}\frac{f'(R(i) - A(i\cdot \delta x - x_c))\cdot A(i)}{f(R(i) - A(i\cdot \delta x - xc))} \tag{a2}$$

The second differentiation is given by

$$\frac{\partial^2 \text{In}\, p(\boldsymbol{R};x_c)}{\partial x_c^2}=\sum_{i=1}^{n_s}\left[\frac{-f'^2(R(i))\cdot A'^2(i)}{f^2(R(i))}+\frac{-f''(R(i)).\ A'^2(i) - f'(R(i))\cdot A''(i)}{f(R(i))}\right) \tag{a3}$$

Since the distribution function of $\beta(i)$ is a well behaved one, its value and the derivative of its self are both zero at infinity, therefore, the integral of both $f'(R(i))$ and $f''(R(i))$ are zero. The expectation of (a3) is then given by

$$E\left(\frac{\partial^2 \ln p(\boldsymbol{R};x_c)}{\partial x_c^2}\right)=-\int_{-\infty}^{\infty}\frac{f'^2(R(i))}{f^2(R(i))}\, dR(i)\cdot\sum_{i=1}^{n_s}A'^2(i) \tag{a4}$$

Using the Cramer Rae's inequality and substitute the summation of $A'^2(i)$ by an integral, the lower bound is found to be

$$\text{var}\{x_c\}\geq\frac{\left(\int_{-00}^{\infty}\frac{f'^2(R(i))}{f(R(i))}\, dR(i)\right)^{-1}}{\sum_{i=1}^{n_s}\left[A'(i\cdot\delta x - x_c)\right]^2} \approx \frac{\left(\int_{-00}^{\infty}\frac{f'^2(R(i))}{f(R(i))}\, dR(i)\right)^{-1}\cdot\delta x}{\int_{-\Delta x_1}^{\Delta x_2}\left[A'(x-x_c)\right]^2 dx} \tag{a5}$$

By Monte Carlo simulation, $(\int_{-\infty}^{\infty} f'^2\ (R(i))\, f'1\ (R(i))dR(i))^{-1}$ is found to be very close to the variance of $f(R(i))$. In addition, it can be proven that $(\int_{-\infty}^{\infty} f'^2(R(i))f^{-1}(R(i))dR(i))^{-1}$ is exactly equal to the variance of $f(R(i))$ if $f(R(i))$ is Gaussian distributed.

REFERENCE

1. Li, F. K., et. al., Doppler parameter estimation for synthetic aperture radar, IEEE. Trans. on Geoscience and Remote Sensing, Vol. 23, pp. 49-56, 1985.
2. Jin, M., Optimal Doppler centroid estimation for SAR data from a quasi-homogenous source, IEEE. Trans. on Geoscience and Remote Sensing, Vol. 24, pp. 1022-1025, May 1986.
3. Madsen, S. N., Estimating the Doppler centroid of SAR data, IEEE. Trans. on Aerosp. Electron. Syst. Vol. 25, pp. 134-140,1989.
4. Chang, C. Y. and Curlander, J. C., Doppler centroid estimation ambiguity for synthetic aperture radars, Proc. IGARSS '89 Symp., pp. 2567-2571.
5. Cheng, T., Jin, M., and Curlander, J., Refinement of Magellan radiometric correction using range centroid estimation, IGARSS '92 Symp., pp. 1167-1170.
6. Eldhuset, K., ScanSAR processing and simulation. CEOS SAR Calibration Workshop, 1993. ESA/ESTEC, Noordwijk, The Netherlands:ESAp.341 346.
7. Luscombe, A, P., Using the overlap regions to improve ScanSAR calibration. CEOS SAR Calibration Workshop, 1993. ESA/ESTEC, Noordwijk, The Netherlands: ESA p. 341346,
8. Swerling, P., Parameter estimation for waveforms in additive Gaussian noise, SIAM J, Vol. 7, pp. 152-166, June, 1959.
9. Cramer, H., Mathematical methods of statistics, Princeton, NJ: Prentice-Hall, 1987.
10. Bamler, R., Doppler frequency estimation and the Cramer-Rao bound, IEEE. Trans. on Geoscience and Remote Sensing, Vol. 29, No. 3, May 1991.
11. Moreira, A., Suppressing the azimuth ambiguities in synthetic aperture radar images, IEEE. Trans. on Geoscience and Remote Sensing, Vol. 31, No. 4, July 1993.